

Fluid coding and coexistence in ultra wide band networks*

Daniele Domenicali · Guerino Giancola ·
Maria-Gabriella Di Benedetto

Published online: 4 May 2006
© Springer Science + Business Media, LLC 2006

Abstract Time Hopping Ultra Wide Band (TH-UWB) commonly encodes the data symbols by shifting the position of the transmitted pulses by a quantity that is quantized over the inter-pulse interval range. In this paper, we relax the hypothesis of a discrete value for the time shift introduced by the TH code, by considering the possibility of generating real-valued codes that introduce time hopping in a “fluid” way. The effect on the power spectral density of generated signals is analyzed, and application of fluid coding to multiple access and to network coexistence is investigated by simulation.

* Portions of this work were presented at the 2005 2nd International Workshop Networking with Ultra Wide Band, Workshop on Ultra Wide Band for Sensor Networks [M.G. Di Benedetto, G. Giancola, D. Domenicali and P. Ingargiola “Fluid Coding in Time Hopping Ultra Wide Band Networks,” Proceedings of the IEEE 2nd International Workshop Networking with Ultra Wide Band—Ultra Wide Band for Sensor Networks, July 2005, Rome, Italy].

D. Domenicali (✉) · G. Giancola · M.-G. Di Benedetto
School of Engineering, University of Rome La Sapienza, Infocom,
Department, Via Eudossiana, 18-00184 Rome, Italy
e-mail: dome@newyork.ing.uniroma1.it

G. Giancola
e-mail: giancola@newyork.ing.uniroma1.it

M.-G. Di Benedetto
e-mail: dibenedetto@newyork.ing.uniroma1.it

Keywords: Ultra Wide Band · Impulse Radio · Time Hopping Coding · Multi-User UWB Communications

1. Introduction

Impulse Radio (IR) is based on the radiation of pulses that are very short in time. This radiation generates signals characterized by an ultra wide bandwidth, called Ultra Wide Band (UWB) signals. Rather than modulating a continuous wave, as is the case in continuous transmissions, the information symbol stream modulates the position, amplitude, or shape of the pulses. Most commonly adopted schemes are Pulse Position Modulation (PPM) and Pulse Amplitude Modulation (PAM) [1, 2]. In order to control the spectrum of the generated signal, the data symbols are encoded using pseudonoise (PN) sequences. In a common approach, the encoded data symbols introduce a time dither on generated pulses leading to the so-called Time-Hopping UWB (TH-UWB). Direct-Sequence Spread Spectrum (DS-SS), that is, amplitude modulation of basic pulses by encoded data symbols, in the IR version, indicated as Direct-Sequence UWB (DS-UWB), also seems particularly attractive [2–6].

The main focus of this paper is on IR-UWB with TH coding. Common implementations of such a transmission scheme foresee the adoption of codes with

periodicity coinciding with the bit repetition interval. The resulting signal is then periodic with a period equal to the bit repetition interval, and therefore power in the Power Spectral Density (PSD) concentrates at peaks located at multiples of the bit repetition frequency. In order to decrease the energy concentration at peaks, one should allow each pulse to assume random positions inside each pulse interval [7], something that cannot be obtained by simply increasing the periodicity of the TH code.

The analysis of the present paper originates from the above observation. We relax the hypothesis of discrete values for the time shift introduced by the TH code, by considering the possibility of introducing time hopping in a “fluid” way based on the generation of real-valued codes. We analyze the effect on the PSD of a generated signal and propose the application of fluid coding to multiple access based on a particular code generation structure that will be further illustrated in the paper.

In order to test and evaluate the application of fluid TH to multiple access we also introduce a scenario of application, and proceed by simulation. The adopted scenario foresees the presence of multiple users in a given geographical area. All users are in visibility and all active users transmit at same fixed power and at a data rate in the order of a few Mbits/s. Each user is identified by a specific code. We analyze the performance of fluid TH vs. standard TH coding, by computing the Bit Error Rate (BER) at each active receiver.

The paper is organized as follows. Section 2 introduces the signal format and related expressions for the PSD. Section 3 focuses on the novel technique of fluid TH. Section 4 analyzes the effect of adopting a fluid TH code on the PSD. The application of fluid TH to multi-user communications in a specific scenario and comparison of performance with standard TH coding is analyzed by simulation in Section 5. Section 6 contains a discussion of the results obtained as well as an overview of possible applications, and in particular coexistence of UWB communication networks.

2. Signal format

A possible transmission scheme of a TH-UWB signal combined with binary PPM is shown in Fig. 1 [7]. Given $\mathbf{b} = (\dots, b_0, b_1, \dots, b_k, b_{k+1}, \dots)$ the binary sequence generated at a rate of $R_b = 1/T_b$ bits/s, a first system introduces redundancy by repeating each bit N_s times and generating a binary sequence $\mathbf{a} = (\dots, b_0, b_0, \dots, b_0, b_1, b_1, \dots, b_1, \dots, b_k, b_k, \dots, b_k, b_{k+1}, b_{k+1}, \dots, b_{k+1}, \dots) = (\dots, a_0, a_1, \dots, a_j, a_{j+1}, \dots)$ at a rate of $R_{cb} = N_s/T_b = 1/T_s$ bits/s. This system is a simple $(N_s, 1)$ block coder that is a repetition coder. A transmission coder applies then an integer-valued code $\mathbf{c} = (\dots, c_0, c_1, \dots, c_j, c_{j+1}, \dots)$ to the binary sequence $\mathbf{a} = (\dots, a_0, a_1, \dots, a_j, a_{j+1}, \dots)$

and generates a new sequence \mathbf{d} . The generic element of the sequence \mathbf{d} is expressed as follows:

$$d_j = c_j T_c + a_j \varepsilon \quad (1)$$

where T_c and ε are constant terms that satisfy, for all c_j , the condition $c_j T_c + \varepsilon < T_s - T_m$ where T_m is the duration of the pulse. T_c is the chip time and one also has, in general, $\varepsilon \ll T_c$.

Note that \mathbf{d} is a real-valued sequence as opposed to \mathbf{a} , which is binary, and to \mathbf{c} , which is integer-valued; in the most common case \mathbf{c} is a pseudorandom code, its generic element c_j being an integer verifying $0 \leq c_j \leq N_h - 1$. Code \mathbf{c} might be periodic, with period indicated by N_p . When $N_p \rightarrow \infty$, the code tends to loose periodicity, while when $N_p = N_s$ the periodicity of the code coincides with the length of the repetition code. This second case is the most commonly adopted in current implementation schemes.

The coded real-valued sequence \mathbf{d} enters a PPM modulator which generates a sequence of Dirac pulses $\delta(t)$ at a rate of $R_p = N_s/T_b = 1/T_s$ pulses/s. These pulses are located at times $jT_s + d_j$, and are therefore shifted in time from “standard” positions jT_s by d_j . In common practice, the shift introduced by the PPM modulator, $a_j \varepsilon$, is much smaller than the shift introduced by the TH code, $c_j T_c$.

Finally the pulse shaper with impulse response $p(t)$, produces a sequence of strictly non-overlapping pulses.

The signal $s(t)$ at the output of the cascade of the above systems can be expressed as follows:

$$s(t) = \sum_{j=-\infty}^{+\infty} p(t - jT_s - c_j T_c - a_j \varepsilon) \quad (2)$$

Note that the bit interval T_b is: $T_b = N_s T_s$. Also note that in Eq. (2), the term $c_j T_c$ defines pulse randomization or dithering with respect to multiples of T_s . We represent $c_j T_c$ by a random TH dither η_j that can be assumed to be distributed between 0 and $T_\eta < T_s - T_m - \varepsilon$, and we obtain:

$$s(t) = \sum_{j=-\infty}^{+\infty} p(t - jT_s - \eta_j - a_j \varepsilon) \quad (3)$$

The global effect of η_j and ε is to introduce a random time shift, distributed between 0 and $T_\eta + \varepsilon < T_s - T_m$, which will be indicated by θ_j leading to the following expression for the transmitted signal:

$$s(t) = \sum_{j=-\infty}^{+\infty} p(t - jT_s - \theta_j) \quad (4)$$

The PSD of signal of Eq. (4), $P_s(f)$, for $N_p = N_s$, can be found under the hypothesis that the time dither process θ , that incorporates the time shift introduced by the TH code η and the time shift introduced by the PPM modulator ε , is a strict-sense stationary discrete random process, where θ_j are the samples of a strict-sense stationary continuous process and the different θ_j are statistically independent with a common probability density function $w(\theta_j)$. One obtains:

$$P_s(f) = \frac{|P(f) \sum_{m=1}^{N_s} e^{-j(2\pi f(mT_s + \eta_m))}|^2}{T_b} \cdot \left[1 - |W(f)|^2 + \frac{|W(f)|^2}{T_b} \sum_{n=-\infty}^{+\infty} \delta\left(f - \frac{n}{T_b}\right) \right] \tag{5}$$

where $P(f)$ is the Fourier Transform of $p(t)$, that is the transfer function of the pulse shaper, and $W(f)$ is the Fourier transform of w coinciding with the characteristic function of w computed in $-2\pi f$:

$$W(f) = \int_{-\infty}^{+\infty} w(s) e^{-j2\pi fs} ds = \langle e^{-j2\pi fs} \rangle = C(-2\pi f) \tag{6}$$

Equation (5) shows the effect of the TH code and of the time shift introduced by the PPM modulator, which follows the characteristics of the statistical properties of the source. Note that the discrete component of the spectrum has lines at $1/T_b$. The amplitude of the lines is weighted by the statistical properties of the source represented by $|W(f)|^2$. If p indicates the probability of emitting a 0 bit (no shift) and $1-p$ the probability of emitting a ‘1’ bit (ε shift), one can write:

$$|W(f)|^2 = 1 + 2p^2(1 - \cos(2\pi f\varepsilon)) - 2p(1 - \cos(2\pi f\varepsilon)) \tag{7}$$

If the source emits equiprobable symbols 0 and 1, then Eq. (7) simplifies as follows:

$$|W(f)|^2 = \frac{1}{2} (1 + \cos(2\pi f\varepsilon)) \tag{8}$$

Note here that ε is small and therefore the discrete components dominate the spectrum. In the simplifying hypothesis that ε is negligible, Eq. (5) is periodic with period $1/T_b$. Note that Eq. (5) can also be applied to any type of source, not necessarily binary.

3. Fluid time-hopping coding

When the discrete-valued $c_j T_c$ term in Eq. (2) and in the transmitter structure of Fig. 1 is replaced by a real value c_j defined in the interval $[0, T_s - T_m - \varepsilon]$, the signal of Eq. (2) becomes:

$$s(t) = \sum_{j=-\infty}^{\infty} p(t - jT_s - c_j - a_j\varepsilon) \tag{9}$$

Note that when going from pseudorandom to fluid coding the parameter N_h becomes irrelevant. In both fluid and discrete cases, codes may be periodic of period N_p .

As obvious, there exists a variety of possible choices for the analog waveform that generates the fluid code. One possible way is to sample a sinewave $c(t)$ expressed as:

$$c(t) = \frac{(T_s - T_m - \varepsilon)}{2} \cdot [1 + \sin(2\pi f_0 t + \varphi)] \tag{10}$$

where the period of the sinewave $1/f_0$ coincides with the period of the code $N_p T_s$, that is $f_0 = 1/(N_p T_s)$. Phase φ falls in the interval $[0, 2\pi]$. We call function $c(t)$ the ‘code function’ and plot an example of it in Fig. 2. Fig. 2 shows in the upper plot the sinewave for a fixed set of parameter values, with the sampling instants located at multiples of T_s . The lower plot of Fig. 2 shows the sequence of pulses that are shifted according to the sampled values of the sinewave that form the fluid coding values.

The generic element c_j of the code is in the sinewave case expressed by:

$$c_j = c(jT_s) = \frac{(T_s - T_m - \varepsilon)}{2} \cdot [1 + \sin(2\pi f_0 jT_s + \varphi)]$$

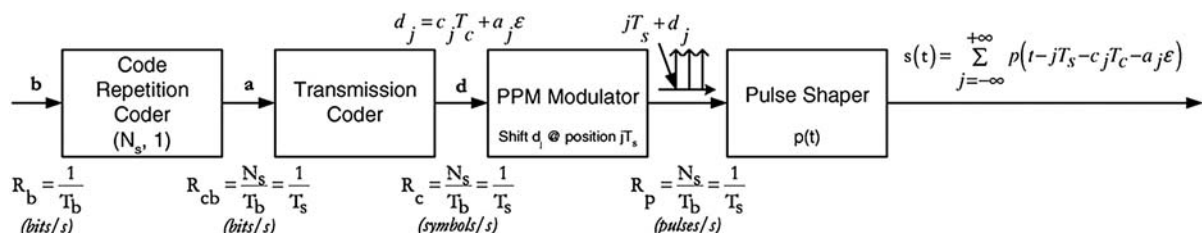


Fig. 1 Transmission scheme for a PPM-TH-UWB signal (from Di Benedetto/Giancola, UNDERSTANDING ULTRA WIDE BAND RADIO FUNDAMENTALS, (c)2005, Chapter 2. Reprinted by permission of Pearson Education, Inc., Upper Saddle River, New Jersey)

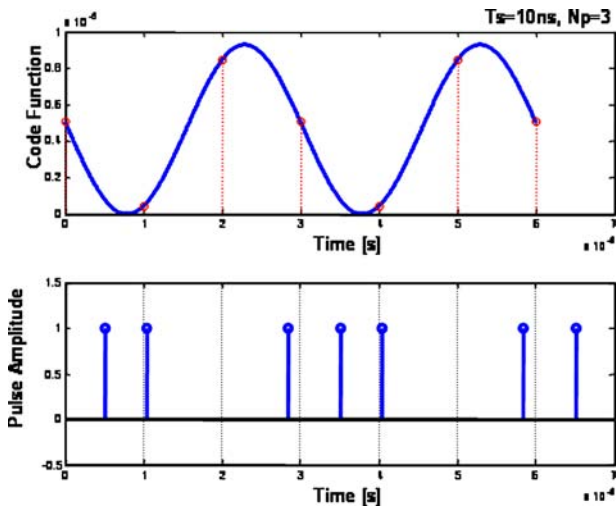


Fig. 2 The upper plot shows a possible code function represented by a sinuswave for $T_s = 10$ ns, $N_p = 3$. The sampling times at multiples of T_s are highlighted. The lower plot shows the train of pulses of a generated signal. Pulse positions are shifted by a fluid value provided by the samples of the code function

$$= \frac{(T_s - T_m - \varepsilon)}{2} \cdot \left[1 + \sin\left(2\pi \frac{j}{N_p} + \varphi\right) \right] \quad (11)$$

c_j is real and is defined in the interval $[0, T_s - T_m - \varepsilon]$. Note that in case of multi-user communications each user can be assigned with different f_0 or φ values. This multiple access scheme will be further discussed in Section 5.

4. Application of fluid time-hopping to spectrum shaping

4.1. Discussion on the effect of fluid TH coding on spectrum shaping

Fluid TH coding may be adopted for removing peaks in the PSD of the transmitted signal, with the beneficial effect of distributing power more evenly over the frequency bandwidth. Fluid TH coding enables, therefore, better management of power, while keeping the PSD of the transmitted signal below spectral masks. An example of the application of fluid TH for increasing transmission power, in single-link communications, is presented in Figs 3 and 4.

Figure 3 represents the PSD of a signal s_1 , with total transmitted power $P_{TOT} = -30$ dBm. Signal s_1 adopts a standard discrete pseudorandom TH code, with average pulse repetition period $T_s = 10$ ns, chip time $T_c = 1$ ns, and code period $N_p = 5000$. As expected, the transmitted power for signal s_1 is concentrated at spectral peaks located at multiples of the repetition frequency of the TH sequence, which is here 1 GHz.

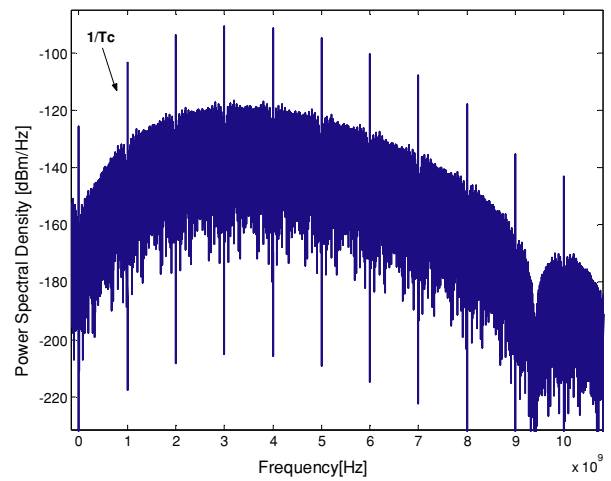


Fig. 3 Power Spectral Density of UWB signal s_1 , with standard discrete TH coding

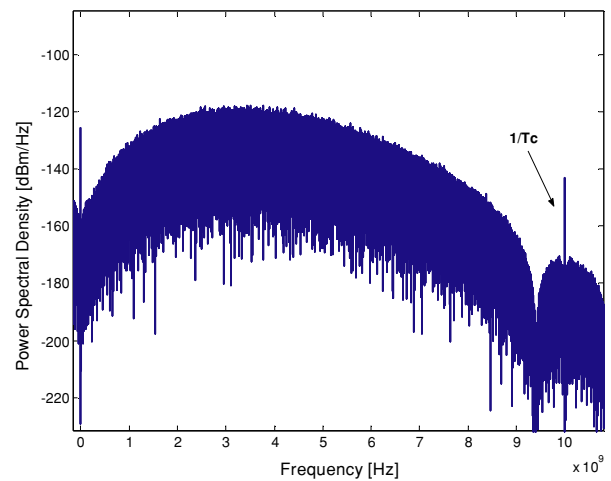


Fig. 4 Power Spectral Density of UWB signal s_2 , with fluid pseudo-random TH coding

Figure 4 represents the PSD of a second UWB signal s_2 , with same average pulse repetition period and same total transmitted power as signal s_1 , but tending to fluid TH coding. This effect is obtained by significantly decreasing T_c while maintaining same T_s . In particular, the PSD of Fig. 4 was obtained by using $T_s = 10$ ns, $T_c = 0.1$ ns. As expected, the introduction of a quasi-fluid TH code has the effect of eliminating peaks in the PSD of the transmitted signal. In particular, we can note on Fig. 4 that peak values of the PSD of signal s_2 are about two orders of magnitude smaller than peak values of s_1 . Under the hypothesis that transmission power P_{TOT} for signal s_1 was determined in order to meet a given set of emission limitations on transmitted PSDs, we can conclude, therefore, that the adoption of a fluid TH code allows a significant increase in the total transmitted power. In the proposed example, in particular, the gain in transmission power allowed by fluid TH ranges in the order of 20 dB. Such an increase of transmission power corresponds to an increase

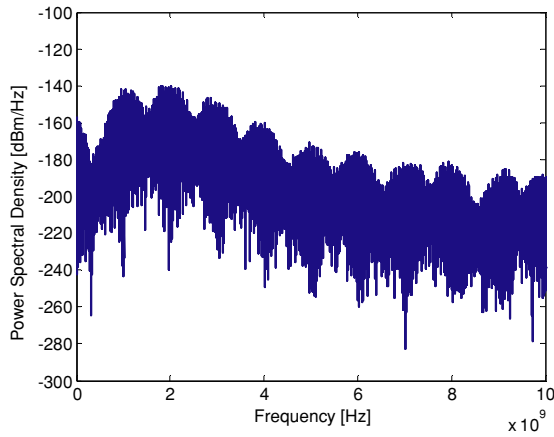


Fig. 5 Power Spectral Density of a UWB signal g_1 , with fluid sinusoidal TH coding ($T_S = 25$ ns and $N_P = 5$)

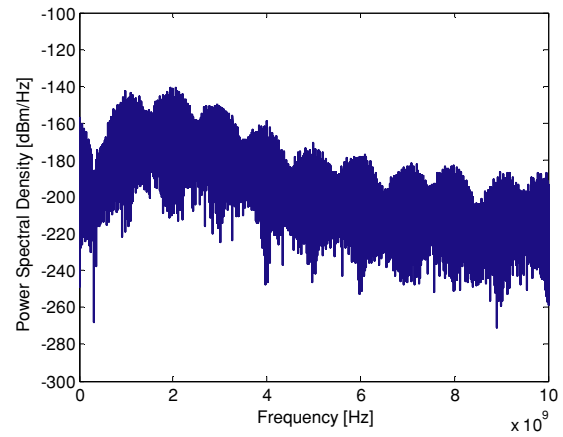


Fig. 7 Power Spectral Density of a UWB signal g_2 , with fluid sinusoidal TH coding ($T_S = 25$ ns and $N_P = 7$)

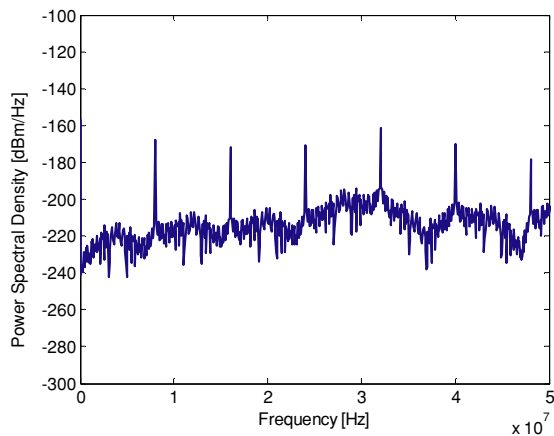


Fig. 6 Zoom of Figure 5: Power Spectral Density of a UWB signal g_1 , with fluid sinusoidal TH coding ($T_S = 25$ ns and $N_P = 5$)

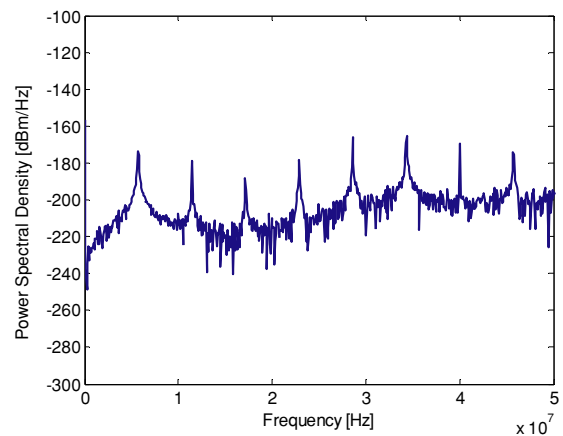


Fig. 8 Zoom of Figure 7: Power Spectral Density of a UWB signal g_2 , with fluid sinusoidal TH coding ($T_S = 25$ ns and $N_P = 7$)

in the transmission range for a given SNR at the receiver, or to a reduced probability of error for a given distance between transmitter and receiver.

5. Application of fluid time hopping to multi-user communications

5.1. Application of sinusoidal fluid coding to multiple access

Figures 5 and 6 represent the PSD of a signal g_1 , that adopts a sinusoidal TH code with $T_S = 25$ ns and $N_P = 5$. In this example, the code repetition period is $N_P T_S = 125$ ns, and spectral lines are thus equally spaced by 8 MHz. Note that spectral peaks are about 20 dB higher than the continuous part of the spectrum. Fig. 6 is a zoomed-in plot of the lower part of the PSD.

Figures 7 and 8 represent the PSD of a signal g_2 , which adopts a sinusoidal TH code with the same T_S value as sig-

nal g_1 , but with an increased value for N_P , which is now $N_P = 7$. In this case, the code repetition period is $N_P T_S = 175$ ns, and spectral lines are thus equally spaced by 5.71 MHz. Similarly to the case of signal g_1 , spectral peaks are about 20 dB higher than the continuous part of the PSD. Fig. 8 is a zoomed-in plot of the lower part of the PSD.

As shown, in the case of sinusoidal code function, the PSD is characterized by spectral lines occurring at multiples of $1/N_P T_S$. As a result, given a pulse repetition period T_S , power concentration in the PSD can be easily governed by proper selection of code period N_P .

Figure 9 compares the two PSDs of signals g_1 and g_2 . Here, we observe that the spectral peaks of the two signals are located at different frequencies. Thus, we expect a reduction of interference between different devices operating over the same bandwidth when proper assignment of code periods among different transmissions is implemented. This multiple access scheme will be analyzed in the next section.

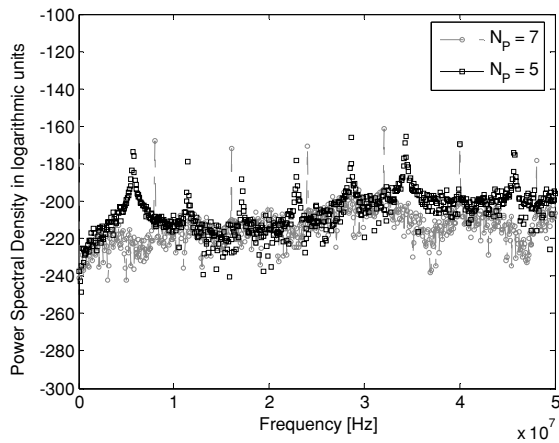


Fig. 9 Comparison of the Power Spectral Density of signals g_1 (gray circles) and g_2 (black squares)

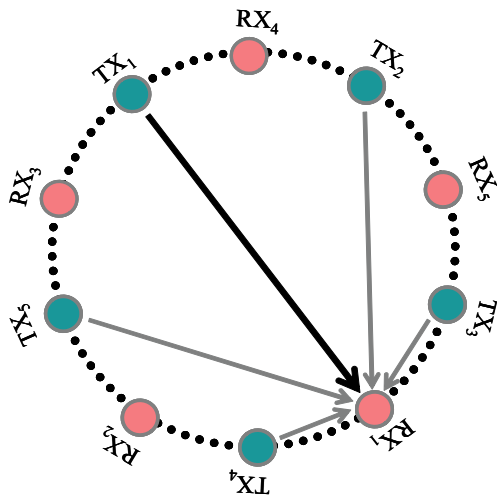


Fig. 10 Ring topology including 10 nodes: nodes are alternately transmitters and receivers. Each transmitter is associated to the diametrically opposed receiver

5.2. Scenario of application

Multiple access and network coexistence can be investigated using a variety of possible topologies, each one capable of underlying different aspects of the system under examination. Though aware of this wide range of different possibilities, our choice was to consider a particular topology, the ring topology, capable of providing a strong inner symmetry and a sort of worst case for the receivers involved as shown in Fig. 10. The nodes forming the ring represent alternately a receiver and a transmitter; each transmitter is associated to the diametrically opposed receiver. In this way, each receiver is put in a critical situation with respect to received useful power and also from a Multi User Interference point of view related to the presence of dominant interferers.

5.3. Settings of the simulation

Two different ring topologies were considered. The first includes 10 nodes (5 transmitters and 5 receivers) while the second one includes 6 nodes (3 transmitters and 3 receivers). Both topologies were characterized by a radius of 10 m and by the following settings: the power of each transmitter was set at 1 mw ; the pulse repetition period T_s was set at 30 ns ; the chip time value T_c for the standard Time Hopping case was set at 5 ns ; the waveform had a duration of approximately 1 ns ; the shift introduced by PPM was set at 2 ns ; each transmitter had a different code periodicity N_p . The pulse was identical for all transmitters with a typical shape of the second derivative of the Gaussian.

Each topology was studied for different values of number of pulses per bit N_s . In particular the performance of the ring topology containing ten nodes was evaluated for five N_s values equally spaced between 2 and 10, while the ring topology with six nodes was examined for N_s assuming five values from 2 to 6. The choice of two different sets of values for N_s is motivated by the fact that the two topologies considered are characterized by a different Multi User Interference situation. For the topology including six nodes, 5 or 6 pulses per bit were in fact sufficient to achieve satisfying BER values for the fluid coding case. Note that increasing the number of pulses per bit results in a decreased bit rate and in an increased energy transmitted per bit. The Signal to Interference Ratio (SIR) also increases when N_s increases; in fact, when SIR is evaluated, the useful contribution rises in a quadratic way with respect to N_s , while the interfering contribution rises in a linear way.

5.4. Simulation results

Results obtained for the ring topology including ten vs. six nodes are shown in Figures 11 and 12, respectively.

6. Discussion and conclusion

In this paper, we analyzed the effect of relaxing the hypothesis of a discrete chip-time on performance of an UWB network adopting TH codes for multiple access. The adoption of a fluid TH code was shown to lead to a more efficient way to deal with emission constraints on transmitted PSDs, if compared to standard discrete TH coding.

We considered a network of asynchronous binary PPM-TH UWB devices using same T_s . Each active link used a specific fluid code known at both transmitter and receiver. Codes were generated by selection of a different period and

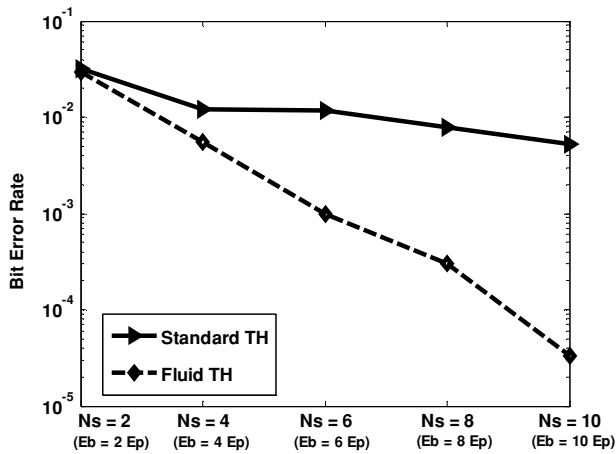


Fig. 11 BER in the two cases of standard TH coding (full line and triangles) and Fluid TH coding (dotted line and lozenges) for the same ring topology (radius = 10 m and 10 nodes) for different values of the number of pulses per bit N_s . The corresponding transmitted energy per bit E_b is also indicated for convenience as a multiple of the energy per pulse $E_p = 1.49 \cdot 10^{-18}$ Joules

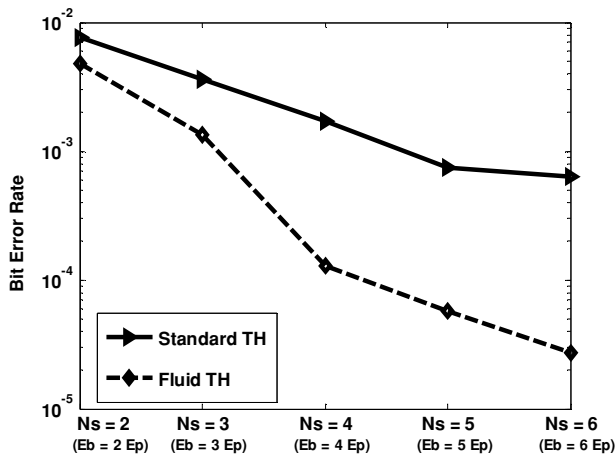


Fig. 12 BER in the two cases of standard TH coding (full line and triangles) and Fluid TH coding (dotted line and lozenges) for the same ring topology (radius = 10 m and 6 nodes) for different values of the number of pulses per bit N_s . The corresponding transmitted energy per bit E_b is also indicated for convenience as a multiple of the energy per pulse $E_p = 1.49 \cdot 10^{-18}$ Joules

random phase of a sine wave for each active link of the network. In this way, spectral peaks of different signals were located at different frequencies.

We focused the analysis on the effect of MUI in the case of a ring topology of nodes where all nodes were in identical MUI conditions. Results indicated that by fluidizing the code a significant improvement in system performance is obtained. These results should be considered as a first ground where fluid TH proves to be effective.

There is in fact a variety of frameworks where fluid TH may be adopted. An extension of the proposed scheme could support a simple clustering function at the MAC level. In clustered MAC networks, nodes are organized in different

subgroups, named *clusters*. Medium access in each cluster is managed independently from other clusters, by defining in general a cluster leader, or *cluster coordinator*, that is in charge of regulating the access of all the other devices of the cluster. In an uncoordinated and asynchronous network, clustering could be easily achieved by separating different clusters with different periods of the sinusoidal fluid TH code. In this way, interference among different subgroups would be better controlled, and cluster coordinators could effectively coordinate access within their cluster without having to take into account interference of devices belonging to foreign clusters.

Fluid TH coding could also be applied with the aim of allowing multiple UWB networks to coexist over the same geographical area. The basic idea, in this case, would be to reduce mutual interference among different networks by adopting a different set of fluid TH codes for each network. Devices belonging to different networks should tune features of the adopted fluid TH codes, such as periodicity, in order to concentrate transmission power at different frequencies. Regarding the single network, resource allocation may still be managed through conventional TH multiple access. One may expect that the advantage of network separation by fluid coding would avoid partitioning the available bandwidth between different networks. With the proposed scheme, network organization may also become dynamic: specific nodes in the network could be in charge of scanning the spectrum at network start-up for locating the best locations in the frequency domain where to concentrate transmission power for all devices. At the end of such a preliminary frequency scanning, all the other nodes of the network would be informed of the specific set of parameters that they must adopt for encoding transmission at the physical layer. Note that the proposed approach does not necessarily imply all networks to adopt the same TH coding scheme. The dynamic and smart operational paradigm might be the privilege of a few sophisticated ones.

One concern that may arise is related to the analogue nature of the code values that may require an increase in complexity of receiver design [8]. In order to solve this question we would like to suggest that the use of analogue correlation and detection might prove to be a feasible way out for low data rate networks. This issue will be the object of future investigation.

Acknowledgment This work was partially supported by the European Union under the 6th Framework Network of Excellence HYCON (contract number FP6-IST-511368) and of Integrated Project P.U.L.S.E.R.S. (project no. 506897)

References

1. M.L. Welborn, System considerations for ultrawideband wireless networks, IEEE Radio and Wireless Conference (Aug. 2001) 5–8.

2. I. Guvenc and H. Arslan, On the modulation options for UWB Systems, *IEEE Military Communications Conference* (Oct. 2003) 892–897.
3. X. Huang and Y. Li, Generating near-white ultra-wideband signals with period extended PN sequences, *IEEE Conference Vehicular Technology Conference 2* (May 2001) 1184–1188.
4. J.R. Foerster, The performance of a direct-sequence spread ultra-wideband system in the presence of multipath, narrowband interference, and multiuser interference, *IEEE Conference on Ultra Wideband Systems and Technologies* (May 2002) 87–91.
5. B.R. Vojcic and R.L. Pickholtz, Direct-sequence code division multiple access for ultra-wide bandwidth impulse radio, *IEEE Military Communications Conference* (Oct. 2003) 898–902.
6. R. Roberts, XtremeSpectrum CFP Document, Available at grouper.ieee.org/groups/802/15/pub/2003/Jul03/03154r3P802-15.TG3a-XtremeSpectrum-CFP-Documentation.pdf (July 2003).
7. M.-G. Di Benedetto and G. Giancola, *Understanding Ultra Wide Band Radio Fundamentals* (Upper Saddle River, New Jersey, Prentice Hall Pearson Education, Inc., 2004).
8. Y.-P. Nakache and A.F. Molisch, Spectral shape of UWB signals—Influence of modulation format, multiple access scheme and pulse shape, *IEEE Vehicular Technology Conference Volume: 4* (April 2003) 2510–2514.



Daniele Domenicali took his Laurea degree in Telecommunications Engineering at the University of Rome La Sapienza in 2004. In November 2004 Domenicali wins the open competition for PhD scholarship in Information and Communication Engineering. He is teaching assistant for the course of “UWB Communication Systems” conducted by Professor Maria Gabriella Di Benedetto at the University of Rome La Sapienza. His

research activity includes Pulse Shaping and the related modulation and coding techniques (Time Hopping Coding, PAM and PPM Modulation). Particular attention is paid to the effects produced in the Power Spectral Density, in order to find solutions capable of optimizing spectrum occupation while meeting the constraints imposed by emission masks. Daniele Domenicali is involved in the European Network of Excellence HYCON (Hybrid Control: Taming Heterogeneity and Complexity of Networked Embedded Systems).



Guerino Giancola received the “Laurea” degree (magna cum laude) in Telecommunications Engineering, and the Ph.D. degree in Information and Communication Engineering from University of Rome La Sapienza, in 2001 and 2005, respectively. He is currently a research affiliate at the INFOCOM Department at University of Rome La Sapienza, where is actually holding the course of “Electrical Communications” for the degree on

Electronic Engineering. His research interests include the analysis and modelling of Multi User Interference in Impulse Radio systems, and the

design of Medium Access Control functions and protocols for UWB ad-hoc networks. Guerino Giancola recently co-authored with Prof. Maria-Gabriella Di Benedetto a book on Ultra Wide Band from radio to the network, titled “Understanding Ultra Wide Band Radio Fundamentals” and published by Prentice Hall in June 2004. He is now involved in the European project “PULSERS – Pervasive Ultra wideband Low Spectral Energy Radio Systems” and in the European Network of Excellence “HYCON- Hybrid Control: Taming Heterogeneity and Complexity of Networked Embedded Systems”. Guerino Giancola is a member of the IEEE Communication Society.



Maria-Gabriella Di Benedetto obtained her Ph.D. in Telecommunications in 1987 from the University of Rome La Sapienza, Italy. In 1991, she joined the Faculty of Engineering of University of Rome La Sapienza, where currently she is a Full Professor of Telecommunications at the Infocom Department. She has held visiting positions at the Massachusetts Institute of Technology, the University of California, Berkeley, and the University of Paris XI, France. In 1994, she received the Mac Kay Professorship award from the University of California, Berkeley.

Her research interests include wireless communication systems and speech science. From 1995 to 2000, she directed four European projects for the design of UWB. Since 2000, she has been active in fostering the development of Ultra Wide Band (UWB) radio communications in Europe. Within the 5th framework, she directed for the Infocom Dept. two European projects (whyless.com and UCAN) aimed at the design and implementation of UWB ad-hoc networks. Currently, within the 6th EU Framework, her “Networking with UWB” research group participates in the PULSERS Integrated Project which will integrate UWB research and development in Europe for the next years, and in the LIAISON Integrated Project as regards the application of UWB to location-based services. She also participates in the HYCON network of excellence. Dr. Di Benedetto is co-edited several Special Issues on UWB communications and networks for several Journals including IEEE JSAC, Journal of Communications and Networks, Mobile Networks and Applications, Eurasip. In 2004, Dr. Di Benedetto co-authored with G. Giancola the first published book on UWB for communications titled “Understanding Ultra Wide Band Radio Fundamentals” and published by Prentice Hall. She recently completed the co-edition of two new books on UWB that will be published by 2005: **UWB Communication Systems - A comprehensive overview**, with T. Kaiser, D. Porcino, A. Molisch, and I. Oppermann, Hindawi Publishing Corporation, 2005, and **Ultra Wideband Wireless Communications** with H. Arslan and Z.N. Chen, John Wiley & Sons, Inc., 2005.